Available online at www.sciencedirect.com
SCIENCE DIRECT
ELSEVIER Computers and Mathematics with Applications 48 (2004) 1135–1151
An International Journal computers & mathematics with applications
www.elsevier.com/locate/camwa

Derivation and Analysis of Near Wall Models for Channel and Recirculating Flows

V. JOHN†
Faculty of Mathematics
Otto-von-Guericke-University
Magdeburg, Germany
john@mathematik.uni-magdeburg.de

W. LAYTON‡ AND N. SAHIN‡
Department of Mathematics
University of Pittsburgh
Pittsburgh, PA 15260, U.S.A.
<wjl><nisst6>@pitt.edu

Abstract—The problem of predicting features of turbulent flows occurs in many applications such as geophysical flows, turbulent mixing, pollution dispersal, and even in the design of artificial hearts. One promising approach is large eddy simulation (LES), which seeks to predict local spatial averages $\bar{\mathbf{u}}$ of the fluid's velocity $\mathbf{u}$. In some applications, the LES equations are solved over moderate time intervals and the core difficulty is associated with modeling near wall turbulence in complex geometries. Thus, one important problem in LES is to find appropriate boundary conditions for the flow averages which depend on the behavior of the unknown flow near the wall. Inspired by early works of Navier and Maxwell, we develop such boundary conditions of the form

$$\bar{\mathbf{u}} \cdot \mathbf{n} = 0 \qquad \text{and} \qquad \beta\left(\delta, \mathrm{Re}, |\bar{\mathbf{u}} \cdot \boldsymbol{\tau}|\right) \bar{\mathbf{u}} \cdot \boldsymbol{\tau} + 2\,\mathrm{Re}^{-1}\, \mathbf{n} \cdot \mathbb{D}\left(\bar{\mathbf{u}}\right) \cdot \boldsymbol{\tau} = 0$$

on the wall. We derive effective friction coefficients β appropriate for both channel flows and recirculating flows and study their asymptotic behavior as the averaging radius $\delta \to 0$ and as the Reynolds number $\mathrm{Re} \to \infty$. In the first limit, no-slip conditions are recovered. In the second, free-slip conditions are recovered. Our goal herein is not to develop new theories of turbulent boundary layers but rather to use existing boundary layer theories to improve numerical boundary conditions for flow averages. © 2004 Elsevier Ltd. All rights reserved.

Keywords—Large eddy simulation, Near wall models, Turbulence, Boundary layers.

1. INTRODUCTION

In the late 1970s, one author (Layton) had the privilege of hearing a lecture by Professor George Fix. At the end of that lecture, George predicted that the next ten years of numerical analysis would be dedicated to computing functionals of solutions of models accurately when it is impossible to compute the solution itself accurately. Characteristically, George's prediction was scientifically accurate, but optimistic in both the starting point and the completion date. In

†Partially supported by the Deutsche Akademische Austauschdienst (D.A.A.D.).
‡Partially supported by NSF Grants DMS 9972622, DMS 0207627, INT 9814115, and INT 9805563.

0898-1221/04/$ - see front matter © 2004 Elsevier Ltd. All rights reserved. Typeset by $\mathcal{A}\mathcal{M}\mathcal{S}$-TEX
doi:10.1016/j.camwa.2004.10.011

this paper, we consider a problem which fits within George's vision: approximate averages of turbulent flows accurately when the fluid velocity itself cannot be accurately simulated.

The problem of predicting the behavior of turbulent flows is ubiquitous in engineering applications. When only long time statistics are needed, carefully calibrated conventional turbulence models are a useful tool. On the other hand, when dynamic features of the flow are needed, large eddy simulation (LES) is one of the preferred techniques. For LES, which seeks to predict local, spatial flow averages above a preassigned length scale δ, to be useful as an engineering design tool, at least two fundamental improvements are needed in current practice. First, for problems with delicate energy balance that must be integrated over long time intervals, better subgrid models are necessary. Such problems often occur in geophysical applications. For problems in complex geometries in which turbulence is caused by interaction between the flow and the walls, better boundary treatments of near wall turbulence are urgently needed. This latter type of problem is very common in engineering practice. Further, if LES is to be used as a part of a design process, the boundary treatments used should not require full griding and resolution of the turbulent boundary layers. Thus, the core difficulties of applying LES usefully in engineering settings include the mathematical question of finding appropriate boundary conditions for flow averages to be used in the simulation. We consider exactly this problem herein.

There is a good deal of computational experience, e.g., [1], and some mathematical support, [2], for the main claim of LES that it can accurately predict the motion of the large (size $\geq O(\delta)$) eddies in a turbulent flow with computational complexity independent of the Reynolds number and depending only on the resolution, δ, sought. For this claim to be true (and within the classical approach to LES) two steps must be successfully carried out. First, the Navier-Stokes equations are locally averaged and an accurate subgrid scale model of the effects of the unresolved small eddies ($\ll O(\delta)$) upon the mean flow $\bar{\mathbf{u}}$ must be constructed. There has been an intense interest and development of such models in the LES community, see, e.g., [1,3,4] for examples, and we will not consider this question herein. Second, accurate boundary conditions (known as near wall models or NWM) for the local flow averages $\bar{\mathbf{u}}$ of motions $\geq O(\delta)$ must be found. If the averaging radius $\delta(\mathbf{x})$ is decreased to zero as $\mathbf{x} \to \partial\Omega$, then $\bar{\mathbf{u}}$ will posses Re-dependent boundary layers and the overall computational complexity must grow with Re, although not as rapidly as for the full Navier-Stokes equations; see, e.g., the work of Vasilyev *et al.* [5]. On the other hand, if δ is fixed (or bounded from below), then $\bar{\mathbf{u}}$ is, in principle, computable with complexity independent of Re. However, with fixed δ, $\bar{\mathbf{u}}$ on the flow domain's boundary $\partial\Omega$ will depend (nonlocally) on the unknown flow in a neighborhood of $\partial\Omega$.

In this report, we develop an improved near wall model for LES along ideas of [6]. Our goal is to develop a physically appropriate NWM which is appropriate not only for simple turbulent channel flows but also will improve LES's performance in more complex heterogeneous mixtures of laminar, transitional, and turbulent flows including recirculation. We shall see in Section 4 that recirculation will require nonlinear boundary conditions.

To develop the ideas, we consider solutions $(\mathbf{u}, p)$ of the nondimensionalized incompressible Navier-Stokes equations

$$\begin{aligned} \mathbf{u}_t - 2\,\mathrm{Re}^{-1}\,\nabla\cdot\mathbb{D}(\mathbf{u}) + (\mathbf{u}\cdot\nabla)\mathbf{u} + \nabla p &= \mathbf{f}, && \text{in } (0,T]\times\Omega,\\ \mathbf{u} &= \mathbf{0}, && \text{on } [0,T]\times\partial\Omega,\\ \nabla\cdot\mathbf{u} &= 0, && \text{in } [0,T]\times\Omega,\\ \mathbf{u}(t=0) &= \mathbf{u}_0. \end{aligned} \tag{1}$$

Here, $\Omega \subset \mathbb{R}^d$, $d = 2, 3$, is a bounded domain, $\mathbf{u} : [0,T]\times\Omega \to \mathbb{R}^d$ is the velocity, $p : (0,T]\times\Omega \to \mathbb{R}$ is the pressure and Re is the Reynolds number. The velocity deformation tensor is given by

$$\mathbb{D}_{ij}(\mathbf{u}) = \frac{1}{2}\left(\frac{\partial u_i}{\partial x_j} + \frac{\partial u_j}{\partial x_i}\right), \qquad \text{for } 1 \leq i, j \leq d.$$

Let

$$g_\delta(\mathbf{x}) = \left(\frac{\gamma}{\delta^2\pi}\right)^{d/2} \exp\left(-\frac{\gamma}{\delta^2}\|\mathbf{x}\|_2^2\right) \tag{2}$$

be the Gaussian filter, where $\gamma > 0$ is typically chosen to be $\gamma = 6$, and $\|\mathbf{x}\|_2$ is the Euclidean norm of $\mathbf{x} \in \mathbb{R}^d$. Having extended all functions outside Ω by zero, the "large eddies" are then defined by convolution

$$\bar{\mathbf{u}} := g_\delta * \mathbf{u} = \int_{\mathbb{R}^d} g_\delta(\mathbf{y} - \mathbf{x})\mathbf{u}(\mathbf{x})\, d\mathbf{x}, \quad \bar{p} := g_\delta * p, \quad \bar{\mathbf{f}} := g_\delta * \mathbf{f}, \quad \text{etc.}$$

Several other filters are also commonly used; see, e.g., [1,3]. Although the correct NWM must ultimately depend on the filter selected, the approach we use can easily be extended to other filters and the Gaussian is the most complex case. When the Navier-Stokes equations are convolved with g_δ and a subgrid scale model is used to replace the Reynolds stress tensor $R := \overline{\mathbf{u}\mathbf{u}} - \bar{\mathbf{u}}\,\bar{\mathbf{u}}$ with a tensor depending only on $\bar{\mathbf{u}}$, a closed system of LES equations results. To solve any such system, $\bar{\mathbf{u}}$ at $\partial\Omega$ must be specified.

The most commonly used boundary condition is $\bar{\mathbf{u}} = \mathbf{0}$ on $\partial\Omega$. It is easy to see that this is not consistent; see Figure 1. It also does not agree with our physical intuition of large eddies: hurricanes and tornadoes do slip along the ground and lose energy as they slip! Motivated by this example and earlier work of Navier [7] and Maxwell [8], we will construct herein NWMs of the form

$$\bar{\mathbf{u}} \cdot \mathbf{n} = 0 \quad \text{and} \quad \beta\bar{\mathbf{u}} \cdot \boldsymbol{\tau}_i + 2\,\mathrm{Re}^{-1}\,\mathbf{n} \cdot \mathbb{D}(\bar{\mathbf{u}}) \cdot \boldsymbol{\tau}_i = 0, \qquad \text{on } \partial\Omega, \tag{3}$$

where $\mathbf{n}$ is the outward unit normal, $\{\boldsymbol{\tau}_1, \ldots, \boldsymbol{\tau}_{d-1}\}$ is an orthonormal system of tangential vectors, and β is the effective friction coefficient which must be specified. We stress that the boundary condition (3) does not enforce equilibrium: time fluctuations of the normal stress at the wall will result through (3) in time fluctuations of the slip velocity.

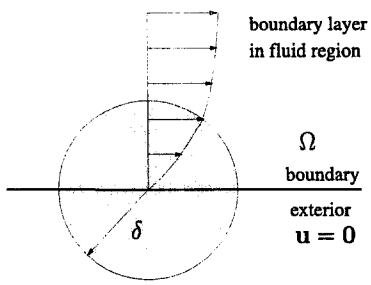

Figure 1. Averaging the velocity at the boundary does not give homogeneous Dirichlet conditions.

Boundary conditions (3) can be implemented easily into a finite-element code; see [9]. In this paper, numerical studies of two- and three-dimensional channel flows across a step are presented which study the influence of the friction parameter on the position of the reattachment point and the reattachment line, respectively, of the recirculating vortex.

Condition (3) is a mathematical expression of no-penetration and slip with resistance. It is often called Navier's slip law [7]. In 1879, Maxwell [8] derived the Navier-Stokes equations from the kinetic theory of gases by an averaging process and recovered the boundary condition (3). In Maxwell's derivation, the friction coefficient β was found to be

$$\beta \sim \frac{\text{microscopic length scale}}{\text{macroscopic length scale}},$$

which is exceedingly small (O(mean free path)) for molecular viscosity in a gas. This early work of Maxwell suggests that for LES we should expect a friction coefficient β scaling like

$$\beta \sim \mathrm{Re}^{-1}\,\frac{L}{\delta}, \qquad L = \mathrm{diam}(\Omega).$$

Such a scaling seems very reasonable since the boundary conditions (3) tend to no-slip conditions as $\delta \to 0$ for fixed Re and to free-slip conditions as $\mathrm{Re} \to \infty$ for fixed δ. For more recent analysis including the boundary conditions (3), see [2,10–12].

As noted above, the behavior of $\bar{\mathbf{u}}$ on $\partial\Omega$ depends on the behavior of $\mathbf{u}$ near $\partial\Omega$. Our analysis presupposes the accuracy of the description of near wall flows. In Section 2, we consider the 2-D laminar case. Since laminar flows can also be underresolved, this case is not without interest and can help to optimize parameter selection in the penalty methods of [13]. In the laminar case, the friction coefficient β is given in (10) and we show

$$\beta(\delta, \mathrm{Re}) \sim \frac{\sqrt{\gamma}}{\delta\,\mathrm{Re}}\Phi(\delta, \mathrm{Re}), \tag{4}$$

where Φ is a function which is uniformly positive and bounded in both δ and Re. Section 3 considers the important question of near wall modeling for 3-D turbulent flows. The optimal friction coefficient is calculated in (19); its asymptotics are again (4) as $\delta \to 0$ for fixed Re and $\mathrm{Re} \to \infty$ for fixed δ, Proposition 3.1. This analysis is for a flow over a flat plate (and thus also over a smoothly curving surface whose curvature is negligible).

Section 4 considers recirculating flows. In such flows there can be a wide variation in local Reynolds numbers. For example, the recirculating flow downstream of a step is much slower than the mean velocity above it. Such flows require a NWM based upon the local Reynolds number, giving a nonlinear friction law. This extension is performed in Section 4.

Numerical tests on a 2-D flow across a step are presented in Section 5. Using a simple LES model, the Smagorinsky model [14], the evolution of the reattachment point is studied for an underresolved flow for which the boundary condition (3) is applied. An improvement of the numerical results using (3) instead of the no-slip boundary condition can be observed.

Some formulas used in Sections 2–4 are collected in the Appendix.

It is important to understand the built-in limitations of any model, and our near wall models are no exception. First, we are replacing an essentially nonlocal condition by a local condition (3) for $\bar{\mathbf{u}}$. Very little is known about well-posedness of nonlocal boundary conditions for the Navier-Stokes equations, so a reduction to a local boundary condition seems necessary. Next, our derivation of the friction coefficient β depends on some knowledge of $\mathbf{u}$ near the walls. Herein we presuppose the accuracy (in the mean) of boundary layer theory. There are situations where simple boundary layer theory should be modified and thus β recalculated. These include flows against a pressure gradient, geometries for which the curvature K of $\partial\Omega$ is nonnegligible, and near stagnation points. Another possibility is to calculate β by postprocessing DNS data or via a calculation of the Navier-Stokes equations near $\partial\Omega$, coupled to an LES model away from Γ, see, e.g., [15].

2. A LAMINAR BOUNDARY LAYER WITH UNIFORM SUCTION IN 2-D

Near wall models are useful in underresolved laminar as well as turbulent flows. Further, the laminar case provides a convenient first validation step and industrial flows often begin laminar and become turbulent through interaction with boundaries. Thus, it is useful to tabulate the friction coefficient in the laminar case, which we do next.

We consider the model situation that $\Omega \subset \mathbb{R}^2$ is the half plane

$$\Omega = \{(x, y),\ y > 0\}.$$

The wall law of a laminar boundary layer on a flat plate is given by

$$\begin{aligned} u &= U_\infty\left(1 - \exp\left(-|V_0|\,\mathrm{Re}\,y\right)\right), && \text{for } y > 0,\\ v &= V_0, && \text{for } y > 0, \end{aligned} \tag{5}$$

see [16, (14.6)], where U_∞ is the free stream velocity and V_0 is a negative constant.

Our aim is to compute the friction coefficient $\beta(\delta, \mathrm{Re})$ for the boundary layer model (5). To this end, u is extended by zero into the lower half plane $\{y < 0\}$ and v is extended by V_0. Since v is a constant function in the whole space, its convolution $\bar{v}$ is constant, too. The outward pointing normal vector on $\partial\Omega = \{y = 0\}$ is $\mathbf{n} = (0, -1)$ and we choose the tangential vector $\boldsymbol{\tau} = (1, 0)$. Hence,

$$\bar{\mathbf{u}} \cdot \boldsymbol{\tau} = \bar{u} \qquad \text{and} \qquad \mathbf{n}^\top \left(2\,\mathrm{Re}^{-1}\,\mathbb{D}\left(\bar{\mathbf{u}}\right)\right) \cdot \boldsymbol{\tau} = -\,\mathrm{Re}^{-1}\,\frac{\partial \bar{u}}{\partial y},$$

and the friction coefficient can be computed by

$$\beta(\delta, \mathrm{Re}) = \mathrm{Re}^{-1}\,\frac{\frac{\partial \bar{u}}{\partial y}(x, 0)}{\bar{u}(x, 0)}. \tag{6}$$

We start by computing $\bar{u}(x, 0)$. Inserting (5), we obtain

$$\begin{aligned}
\bar{u}(x, y) &= g_\delta * u(x, y) \\
&= U_\infty \frac{\gamma}{\delta^2 \pi} \int_{-\infty}^{\infty} \exp\left(-\frac{\gamma}{\delta^2}(x - x')^2\right) dx' \\
&\quad \times \left[\int_0^\infty \exp\left(-\frac{\gamma}{\delta^2}(y - y')^2\right) dy' - \int_0^\infty \exp\left(-\left(\frac{\gamma}{\delta^2}(y - y')^2 + |V_0|\,\mathrm{Re}\,y'\right)\right) dy'\right].
\end{aligned}$$

This integral can be evaluated using (27), (28), and (31) (see the Appendix) leading to

$$\begin{aligned}
\bar{u}(x, y) = \frac{U_\infty}{2} \Bigg\{ &\left[1 + \mathrm{erf}\left(\frac{\sqrt{\gamma}}{\delta} y\right)\right] \\
&- \exp\left(\frac{V_0^2\,\mathrm{Re}^2\,\delta^2}{4\gamma} - |V_0|\,\mathrm{Re}\,y\right) \left[1 - \mathrm{erf}\left(\frac{|V_0|\,\mathrm{Re}\,\delta}{2\sqrt{\gamma}} - \frac{\sqrt{\gamma}}{\delta} y\right)\right]\Bigg\}.
\end{aligned} \tag{7}$$

In particular, we have

$$\bar{u}(x, 0) = \frac{U_\infty}{2} \left\{1 - \exp\left(\frac{V_0^2\,\mathrm{Re}^2\,\delta^2}{4\gamma}\right) \left[1 - \mathrm{erf}\left(\frac{|V_0|\,\mathrm{Re}\,\delta}{2\sqrt{\gamma}}\right)\right]\right\}. \tag{8}$$

The numerator in (6) can be computed directly from (7) using (29). We obtain

$$\begin{aligned}
\frac{\partial \bar{u}}{\partial y}(x, y) = \frac{U_\infty}{2} \Bigg\{ &\frac{2\sqrt{\gamma}}{\delta\sqrt{\pi}} \exp\left(-\frac{\gamma}{\delta^2} y^2\right) \\
&+ |V_0|\,\mathrm{Re} \exp\left(\frac{V_0^2\,\mathrm{Re}^2\,\delta^2}{4\gamma} - |V_0|\,\mathrm{Re}\,y\right) \left[1 - \mathrm{erf}\left(\frac{|V_0|\,\mathrm{Re}\,\delta}{2\sqrt{\gamma}} - \frac{\sqrt{\gamma}}{\delta} y\right)\right] \\
&- \frac{2\sqrt{\gamma}}{\delta\sqrt{\pi}} \exp\left(\frac{V_0^2\,\mathrm{Re}^2\,\delta^2}{4\gamma} - |V_0|\,\mathrm{Re}\,y\right) \exp\left(-\left(\frac{|V_0|\,\mathrm{Re}\,\delta}{2\sqrt{\gamma}} - \frac{\sqrt{\gamma}}{\delta} y\right)^2\right)\Bigg\},
\end{aligned}$$

which gives

$$\frac{\partial \bar{u}}{\partial y}(x, 0) = \frac{U_\infty}{2} |V_0|\,\mathrm{Re} \exp\left(\frac{V_0^2\,\mathrm{Re}^2\,\delta^2}{4\gamma}\right) \left[1 - \mathrm{erf}\left(\frac{|V_0|\,\mathrm{Re}\,\delta}{2\sqrt{\gamma}}\right)\right]. \tag{9}$$

The friction coefficient for the laminar boundary layer wall law is, using (8) and (9),

$$\beta(\delta, \mathrm{Re}) = |V_0| \left\{\frac{1}{1 - \exp\left(V_0^2\,\mathrm{Re}^2\,\delta^2/(4\gamma)\right)\left[1 - \mathrm{erf}\left(|V_0|\,\mathrm{Re}\,\delta/(2\sqrt{\gamma})\right)\right]} - 1\right\}. \tag{10}$$

Note that $\beta(\delta, \mathrm{Re})/|V_0|$ depends only on $|V_0|\,\mathrm{Re}\,\delta/(2\sqrt{\gamma})$.

PROPOSITION 2.1. *Let $\beta(\delta, \mathrm{Re})$ be given as in (10). For fixed Reynolds number* Re, *we have*

$$\lim_{\delta\to 0} \delta\beta(\delta, \mathrm{Re}) = \frac{\sqrt{\pi}\sqrt{\gamma}}{\mathrm{Re}}, \qquad \textit{consequently} \lim_{\delta\to 0} \beta(\delta, \mathrm{Re}) = \infty, \tag{11}$$

and for fixed filter width δ,

$$\lim_{\mathrm{Re}\to\infty} \mathrm{Re}\,\beta(\delta, \mathrm{Re}) = \frac{2\sqrt{\gamma}}{\delta\sqrt{\pi}}, \qquad \textit{consequently} \lim_{\mathrm{Re}\to\infty} \beta(\delta, \mathrm{Re}) = 0. \tag{12}$$

PROOF. Since

$$\lim_{\delta\to 0} \exp\left(\frac{V_0^2\,\mathrm{Re}^2\,\delta^2}{4\gamma}\right)\left[1 - \mathrm{erf}\left(\frac{|V_0|\,\mathrm{Re}\,\delta}{2\sqrt{\gamma}}\right)\right] = 1,$$

the denominator in the first term in (10) tends to zero. To prove (11), multiply $\beta(\delta, \mathrm{Re})$ by δ and write the product as one fraction. Then, (11) follows by an application of the rule of Bernoulli-l'Hospital.

To prove (12), we first note that an application of the rule of Bernoulli-l'Hospital gives

$$\lim_{x\to\infty} \exp\left(x^2\right)\left[1 - \mathrm{erf}\,(x)\right] = 0, \tag{13}$$

$$\lim_{x\to\infty} x\exp\left(x^2\right)\left[1 - \mathrm{erf}\,(x)\right] = \frac{1}{\sqrt{\pi}}. \tag{14}$$

First, multiply $\beta(\delta, \mathrm{Re})$ by $\mathrm{Re}\,\delta/(2\sqrt{\gamma})$ and write the product as one fraction. Using (13) with $x = |V_0|\,\mathrm{Re}\,\delta/(2\sqrt{\gamma})$, one obtains that the denominator of this fraction tends to one. The numerator has such a form that (14) can be applied. ∎

The asymptotic behaviors are illustrated in Figure 2.

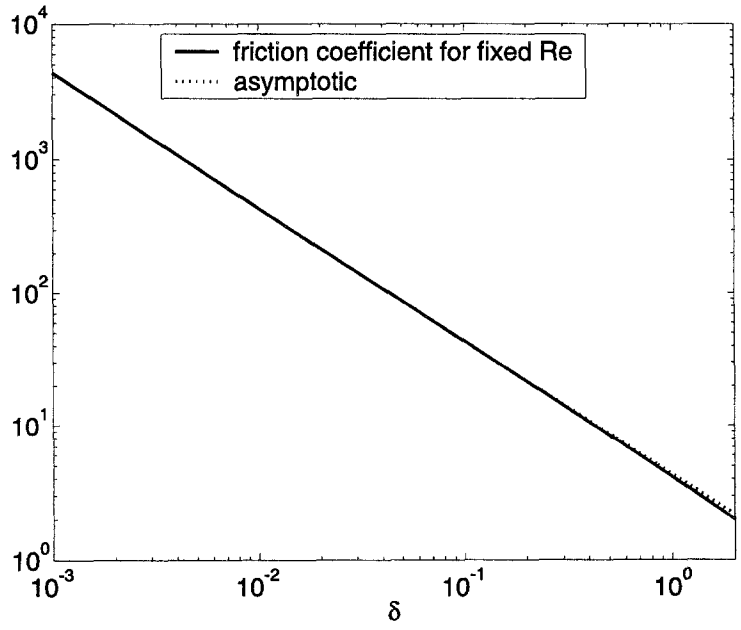

(a). Behavior of $\beta(\delta, \mathrm{Re})$ with respect to δ for constant Re$(= 1)$, $\gamma = 6$, $V_0 = -1$.

Figure 2. Laminar boundary layer, behavior of $\beta(\delta, \mathrm{Re})$ with respect to Re for constant $\delta(= 1)$, $\gamma = 6$, $V_0 = -1$.

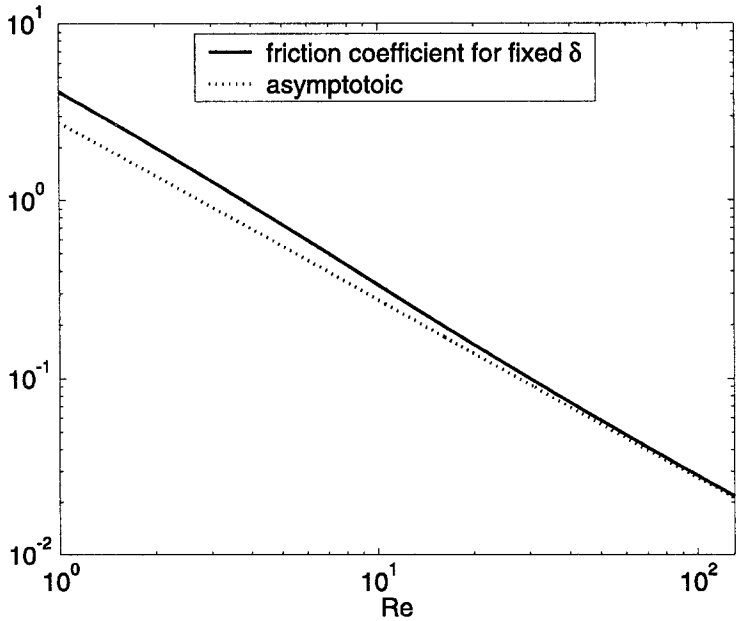

(b). Behavior of $\beta(\delta, \mathrm{Re})$ with respect to Re for constant $\delta(=1)$, $\gamma = 6$, $V_0 = -1$.

Figure 2. (cont.)

REMARK 2.1. The friction laws we derive herein and in the following section are linear and thus not appropriate for recirculating flows. Nevertheless, they are necessary steps to deriving in Section 4 the nonlinear friction laws for recirculating flows.

Formulas (11) and (12) agree with the formula $\beta \sim \mathrm{Re}^{-1} L/\delta$ of Maxwell. Further, they give important insight into parameter selection in penalty methods for imposing the no-slip condition weakly. Formula (11) suggests that the penalty parameter ϵ in the methods of, e.g., [13,17] should be

$$\epsilon \cong (h\,\mathrm{Re})^{-1}\left(\sqrt{\pi\delta}\right)$$

where h is the local mesh width near $\partial\Omega$.

3. THE $1/\alpha^{\mathrm{th}}$ POWER LAW IN 3-D

Next we consider the case of a turbulent boundary layer. There are various theories of turbulent boundary layer, e.g., [3,16,18]. Although the calculation can be done for other descriptions, we perform it herein for power law layers (which is in accord with current views in the subject [18]).

Consider the flat plane $\{(x,y,z) : x \geq 0,\ y = 0\} \subset \mathbb{R}^3$. The velocity $\mathbf{u} = (u,v,w)$ obeys the $1/\alpha^{\mathrm{th}}$ power law, $\alpha > 1$, see [16, (21.4)], provided (time or ensemble averages of) the velocity is given by

$$u = \begin{cases} U_\infty \left(\dfrac{y}{\eta}\right)^{1/\alpha}, & 0 \leq y \leq \eta, \\ U_\infty, & \eta < y, \end{cases} \qquad v = w = 0, \quad \text{for } 0 \leq y,$$

where the boundary layer thickness $\eta = \eta(x)$ is, see [16, (21.8)],

$$\eta(x) = 0.37x\,(U_\infty x\,\mathrm{Re})^{-1/5}, \qquad x \geq 0,$$

and U_∞ is the free stream velocity. One of the most common laws is given by $\alpha = 7$.

We consider the model situation of a reference plate of nondimensional length one. Let $\Omega \subset \mathbb{R}^3$ be the half space

$$\Omega = \left\{(x,y,z) \in \mathbb{R}^3,\ y > 0\right\}.$$

Thus, $\partial\Omega$ is the plane $\{y = 0\}$. In order to handle this situation, we have to eliminate the x-dependence in η by averaging in the x-direction. Since the problem is nondimensionalized, the x-length is thus one. Define an averaged boundary layer thickness by

$$\tilde{\eta} = \int_0^1 \eta(x)\,dx = \frac{37}{180}(U_\infty \operatorname{Re})^{-1/5} = c_\eta \operatorname{Re}^{-1/5}. \tag{15}$$

Now, we define an x-averaged velocity by

$$u = \begin{cases} U_\infty \left(\dfrac{y}{\tilde{\eta}}\right)^{1/\alpha}, & 0 \le y \le \tilde{\eta}, \\ U_\infty, & \tilde{\eta} < y, \end{cases} \qquad v = w = 0, \quad \text{for } 0 \le y.$$

Let $\mathbf{n} = (0, -1, 0)$ be the outward pointing normal vector with respect to Ω on $\{y = 0\}$ and $\boldsymbol{\tau}_1 = (1, 0, 0)$, $\boldsymbol{\tau}_2 = (0, 0, 1)$ be an orthonormal system of tangential vectors. All velocity components are extended by zero outside Ω. We have obviously $\bar{v} = \bar{w} = 0$ and the slip with friction boundary condition (3) thus simplifies to

$$\beta(\delta, \operatorname{Re})\bar{u} - \operatorname{Re}^{-1}\frac{\partial \bar{u}}{\partial y} = 0, \qquad \text{on } \{y = 0\},$$

thus,

$$\beta(\delta, \operatorname{Re}) = \operatorname{Re}^{-1}\frac{\frac{\partial \bar{u}}{\partial y}(x, 0, z)}{\bar{u}(x, 0, z)}. \tag{16}$$

We obtain, using (26), (27), and (34),

$$\begin{aligned}
\bar{u}(x, 0, z) &= (g_\delta * u)(x, 0, z) \\
&= U_\infty \left(\frac{\gamma}{\delta^2 \pi}\right)^{3/2} \\
&\quad \times \left[\int_0^{\tilde{\eta}} \left(\frac{y'}{\tilde{\eta}}\right)^{1/\alpha} \exp\left(-\frac{\gamma}{\delta^2}(y')^2\right) dy' \int_{-\infty}^{\infty} \exp\left(-\frac{\gamma}{\delta^2}(x')^2\right) dx' \right. \\
&\quad \cdot \int_{-\infty}^{\infty} \exp\left(-\frac{\gamma}{\delta^2}(z')^2\right) dz' \\
&\quad \left. + \int_{\tilde{\eta}}^{\infty} \exp\left(-\frac{\gamma}{\delta^2}(y')^2\right) dy' \int_{-\infty}^{\infty} \exp\left(-\frac{\gamma}{\delta^2}(x')^2\right) dx' \int_{-\infty}^{\infty} \exp\left(-\frac{\gamma}{\delta^2}(z')^2\right) dz' \right] \\
&= \frac{U_\infty}{2}\left\{\left(\frac{1}{\pi}\right)^{1/2}\left(\frac{\delta}{\sqrt{\gamma}\tilde{\eta}}\right)^{1/\alpha}\left[\Gamma\left(\frac{\alpha+1}{2\alpha}\right) - \Gamma\left(\frac{\alpha+1}{2\alpha}, \left(\frac{\sqrt{\gamma}\tilde{\eta}}{\delta}\right)^2\right)\right]\right. \\
&\quad \left. + \left[1 - \operatorname{erf}\left(\frac{\sqrt{\gamma}\tilde{\eta}}{\delta}\right)\right]\right\}.
\end{aligned} \tag{17}$$

To compute the numerator in (16), we note first that differentiation and convolution commute because the functions have been extended off the flow domain so as to retain one weak L^2 derivative, i.e.,

$$\frac{\partial \bar{u}}{\partial y} = g_\delta * \frac{\partial u}{\partial y}.$$

A straightforward computation using (26), (27), and (34) gives

$$\begin{aligned}\frac{\partial \bar{u}}{\partial y}(x,0,z) &= g_\delta * \frac{\partial u}{\partial y}(x,0,z)\\ &= U_\infty \left(\frac{\gamma}{\delta^2\pi}\right)^{3/2}\\ &\quad\times\left[\int_0^{\tilde{\eta}} \frac{1}{\alpha}\left(\frac{1}{\tilde{\eta}}\right)^{1/\alpha} (y')^{1/\alpha-1}\exp\left(-\frac{\gamma}{\delta^2}(y')^2\right)\,dy' \int_{-\infty}^{\infty}\exp\left(-\frac{\gamma}{\delta^2}(x')^2\right)\,dx'\right.\\ &\quad\left.\times\int_{-\infty}^{\infty}\exp\left(-\frac{\gamma}{\delta^2}(z')^2\right)\,dz'\right]\\ &= \frac{U_\infty}{2\alpha}\left(\frac{\gamma}{\delta^2\pi}\right)^{1/2}\left(\frac{\delta}{\sqrt{\gamma}\tilde{\eta}}\right)^{1/\alpha}\left[\Gamma\left(\frac{1}{2\alpha}\right)-\Gamma\left(\frac{1}{2\alpha},\gamma\left(\frac{\tilde{\eta}}{\delta}\right)^2\right)\right].\end{aligned} \tag{18}$$

The slip coefficient $\beta(\delta,\mathrm{Re})$ given in (16) can now be computed by (17) and (18)

$$\begin{aligned}\beta(\delta,\mathrm{Re}) &= \mathrm{Re}^{-1}\frac{\gamma^{1/2}}{\alpha\delta}\times\left[\Gamma\left(\frac{1}{2\alpha}\right)-\Gamma\left(\frac{1}{2\alpha},\left(\frac{\sqrt{\gamma}\tilde{\eta}}{\delta}\right)^2\right)\right]\\ &\left\{\left[\Gamma\left(\frac{\alpha+1}{2\alpha}\right)-\Gamma\left(\frac{\alpha+1}{2\alpha},\left(\sqrt{\gamma}\frac{\tilde{\eta}}{\delta}\right)^2\right)\right]+\pi^{1/2}\left(\frac{\sqrt{\gamma}\tilde{\eta}}{\delta}\right)^{1/\alpha}\left[1-\mathrm{erf}\left(\frac{\sqrt{\gamma}\tilde{\eta}}{\delta}\right)\right]\right\}^{-1}.\end{aligned} \tag{19}$$

REMARK 3.1. Considering the $1/\alpha^{\text{th}}$ power law in 2-D under the same geometric situation as in Section 2 gives the same results as in 3-D, i.e., $\bar{u}(x,0)$ is equal to expression (17) and $\frac{\partial \bar{u}}{\partial y(x,0)}$ is equal to expression (18).

PROPOSITION 3.1. *Let $\beta(\delta,\mathrm{Re})$ be given as in (19). If* Re *is constant, then*

$$\lim_{\delta\to 0}\delta\beta(\delta,\mathrm{Re}) = \frac{\sqrt{\gamma}}{\alpha\,\mathrm{Re}}\frac{\Gamma(1/(2\alpha))}{\Gamma((\alpha+1)/(2\alpha))}, \qquad \textit{consequently } \lim_{\delta\to 0}\beta(\delta,\mathrm{Re}) = \infty. \tag{20}$$

If δ is constant, then

$$\lim_{\mathrm{Re}\to\infty}\mathrm{Re}\,\beta(\delta,\mathrm{Re}) = \frac{2\sqrt{\gamma}}{\delta\sqrt{\pi}}, \qquad \textit{consequently } \lim_{\mathrm{Re}\to\infty}\beta(\delta,\mathrm{Re}) = 0. \tag{21}$$

PROOF. From (33) and by the definition of the Gamma function follows

$$\lim_{x\to 0}(\Gamma(a)-\Gamma(a,x)) = \lim_{x\to 0}\int_0^x \exp(-t)t^{a-1}\,dt = 0, \tag{22}$$

$$\lim_{x\to\infty}(\Gamma(a)-\Gamma(a,x)) = \lim_{x\to\infty}\int_0^x \exp(-t)t^{a-1}\,dt = \Gamma(a). \tag{23}$$

Let Re be fixed and consider the last factor in (19). The application of (23) gives that the numerator tends to $\Gamma(1/(2\alpha))$ as $\delta\to 0$ and the first term of the denominator tends to $\Gamma((\alpha+1)/(2\alpha))$. Applying three times the rule of Bernoulli-l'Hospital proves

$$\lim_{x\to 0}\left(\frac{1}{x}\right)^{1/\alpha}\left[1-\mathrm{erf}\left(\frac{a}{x}\right)\right] = 0, \qquad a>0.$$

Thus, the second term in the denominator tends to zero and hence the last factor in (19) tends to $\Gamma(1/(2\alpha))/\Gamma((\alpha+1)/(2\alpha))$. This proves (20).

Also, (21) can be proved by the rule of Bernoulli-l'Hospital. The differentiation of the Gamma and the incomplete Gamma function uses (33) and the rule for differentiating integrals with respect to the upper boundary. The derivative of the error function is obtained by (29). If the numerator and the denominator of the fraction, which is obtained as result of the rule of Bernoulli-l'Hospital, are multiplied with an appropriate power of Re, (21) follows by collecting terms. ∎

The asymptotic behaviors in the case $\alpha = 7$ are illustrated in Figure 3.

REMARK 3.2. It is interesting that the limiting forms of the optimal linear friction coefficient are similar in the 3-D turbulent case to the ones in the 2-D laminar case. In some sense, this dimension independence indicates that the slip with friction condition (3) is the appropriate one and δ and Re are the correct variables for the analysis.

4. A NEAR WALL MODEL FOR RECIRCULATING FLOWS

The previous sections derived linear near wall models (i.e., friction coefficients β) based upon a global Reynolds number. In recirculating flows, there are usually large differences between reference velocities in the free stream and in the recirculation regions. Thus, a linear NWM will tend to overpredict the friction in attached eddies and underpredict it away from attached eddies. The solution of this difficulty is to base the NWM upon the local Reynolds number as follows.

The derivations in Sections 2 and 3 reveal that the predicted local slip velocity, $\bar{\mathbf{u}} \cdot \hat{\boldsymbol{\tau}}$, is a monotone function of Re. Thus, the relationship can be inverted and inserted into the appropriate place in the derivation of the NWM to give a β which depends on the local slip speed, $\beta = \beta(\delta, |\bar{\mathbf{u}} \cdot \hat{\boldsymbol{\tau}}|)$.

To carry out this program, we suppose the $1/7^{\text{th}}$ power law holds. The calculations in Section 3 reveal that the tangential velocity (17) can be written in the form

$$\begin{aligned} \bar{\mathbf{u}} \cdot \boldsymbol{\tau}_1 &= \frac{U_\infty}{2} \left\{ \left(\frac{1}{\pi}\right)^{1/2} \left(\frac{1}{\xi}\right)^{1/7} \left[\Gamma\left(\frac{4}{7}\right) - \Gamma\left(\frac{4}{7}, \xi^2\right)\right] + [1 - \operatorname{erf}(\xi)] \right\} \\ &= g(\xi) \end{aligned} \tag{24}$$

with

$$\xi = \frac{\sqrt{\gamma}\tilde{\eta}}{\delta} = \frac{\sqrt{\gamma} c_\eta}{\delta \operatorname{Re}^{1/5}} > 0.$$

One finds

$$\frac{d\bar{\mathbf{u}} \cdot \boldsymbol{\tau}_1}{d\xi} = g'(\xi) = -\frac{U_\infty}{14\sqrt{\pi}} \left(\frac{1}{\xi}\right)^{8/7} \left[\Gamma\left(\frac{4}{7}\right) - \Gamma\left(\frac{4}{7}, \xi^2\right)\right] < 0.$$

This proves the following lemma.

LEMMA 4.1. *Let $\bar{\mathbf{u}} \cdot \boldsymbol{\tau}_1$ be given by (24). Then, $\bar{\mathbf{u}} \cdot \boldsymbol{\tau}_1$ is a strictly monotone decreasing function of ξ, hence a strictly monotone increasing of* Re. *Thus, an inverse function $\xi = g^{-1}(|\bar{\mathbf{u}} \cdot \boldsymbol{\tau}_1|)$ exists.*

An ideal NWM can thus be obtained by inverting this inverse function for Re in (19): $\beta = \beta(\delta, g^{-1}(|\bar{\mathbf{u}} \cdot \hat{\boldsymbol{\tau}}|))$. However, this is not easily used in practical calculations. Thus, we shall develop an accurate and simple approximate inverse to $g(\xi)$ which still captures the correct double asymptotics. The idea to obtain a usable nonlinear friction coefficient consists in finding an approximation $\tilde{g}(\xi)$ of $g(\xi)$ which can be easily inverted and replace ξ and Re in (19) by $\tilde{g}^{-1}(\bar{\mathbf{u}} \cdot \boldsymbol{\tau}_1)$.

A careful examination of $g(\xi)$ reveals that an appropriate approximation over $0 \le \xi \le \infty$ is of the form

$$\bar{\mathbf{u}} \cdot \boldsymbol{\tau}_1 \approx \frac{U_\infty}{2} \exp\left(-a\xi^b\right), \qquad a, b > 0.$$

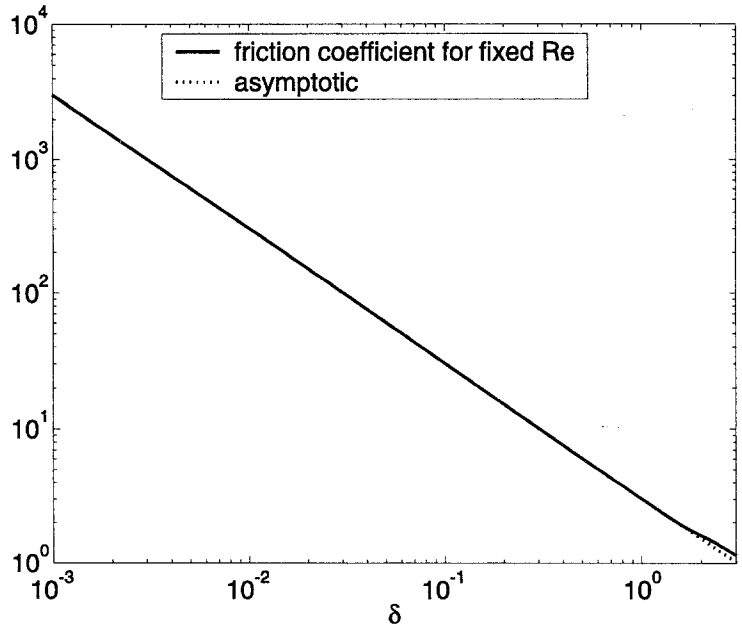

(a). Behavior of $\beta(\delta, \mathrm{Re})$ with respect to δ for constant $\mathrm{Re}(=1)$, $\tilde{\eta}(=1)$, $\gamma = 6$.

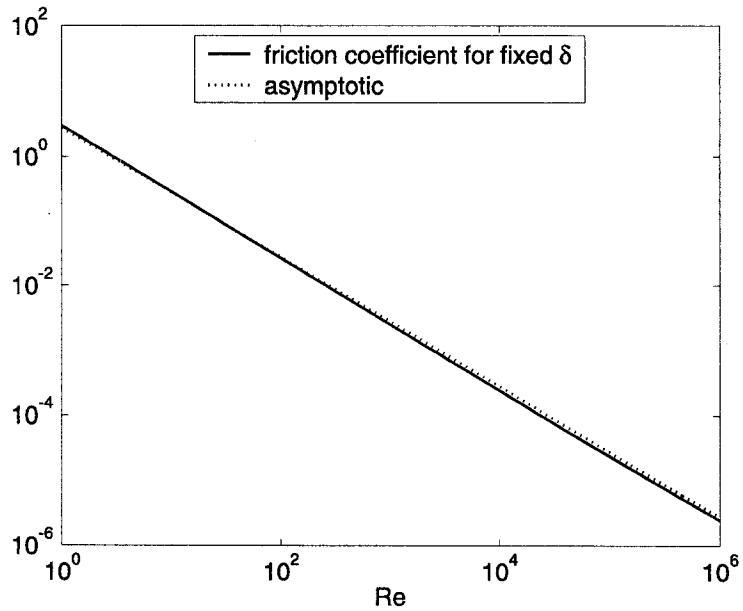

(b). Behavior of $\beta(\delta, \mathrm{Re})$ with respect of Re for constant $\delta(=1)$, $c_\eta = 1$, $\gamma = 6$.

Figure 3. $1/7^{\text{th}}$ power law boundary layer.

This gives

$$\xi = \left(-\frac{1}{a}\ln\left(\frac{2}{U_\infty}(\bar{\mathbf{u}}\cdot\tau_1)\right)\right)^{1/b}, \qquad \mathrm{Re} = \left(\frac{\sqrt{\gamma}c_\eta}{\delta\xi}\right)^5.$$

The constants a and b have to be chosen such that the approximation of (24) is the best in least squares sense: find $a, b > 0$ such that

$$\int_{\xi_l}^{\xi_r} \left[\left(\frac{1}{\pi}\right)^{1/2} \left(\frac{1}{\xi}\right)^{1/7} \left(\Gamma\left(\frac{4}{7}\right) - \Gamma\left(\frac{4}{7}, \xi^2\right)\right) + [1 - \operatorname{erf}(\xi)] - \exp\left(-a\xi^b\right) \right]^2 d\xi \to \min. \quad (25)$$

The left boundary ξ_l and the right boundary ξ_r of the integral have to be specified on the data of the given problem. If they are given, the optimal parameters can be approximated numerically. Such an approximation can be obtained in the following way. The interval $[\xi_l, \xi_r]$ is divided into N equal distance subintervals $[\xi_i, \xi_{i+1}]$ with $\xi_0 = \xi_l$ and $\xi_N = \xi_r$. Then, (25) is replaced by: find $a, b > 0$ such that

$$\sum_{i=0}^{N} \left[\left(\frac{1}{\pi}\right)^{1/2} \left(\frac{1}{\xi_i}\right)^{1/7} \left(\Gamma\left(\frac{4}{7}\right) - \Gamma\left(\frac{4}{7}, \xi_i^2\right)\right) + [1 - \operatorname{erf}(\xi_i)] - \exp\left(-a\xi_i^b\right) \right]^2 \to \min.$$

The necessary condition for a minimum, that the derivatives with respect to a and b vanish, leads to a nonlinear system of two equations. This can be solved iteratively, e.g., by Newton's method. We give some examples for optimal parameters for some intervals in Table 1. These parameters were computed with $N = 50000$ using Newton's method. An illustration of the approximation is presented in Figure 4.

Table 1. Optimal parameters in (25) for different intervals $[\xi_l, \xi_r]$.

ξ_l	ξ_r	a	b
0	0.1	0.142864	1.00312
0	1	0.137149	0.961851
0	10	0.154585	0.497275
0	100	0.238036	0.268180
0	1000	0.342360	0.174579
0	10^6	0.689473	0.0812879
1	10	0.170289	0.444825

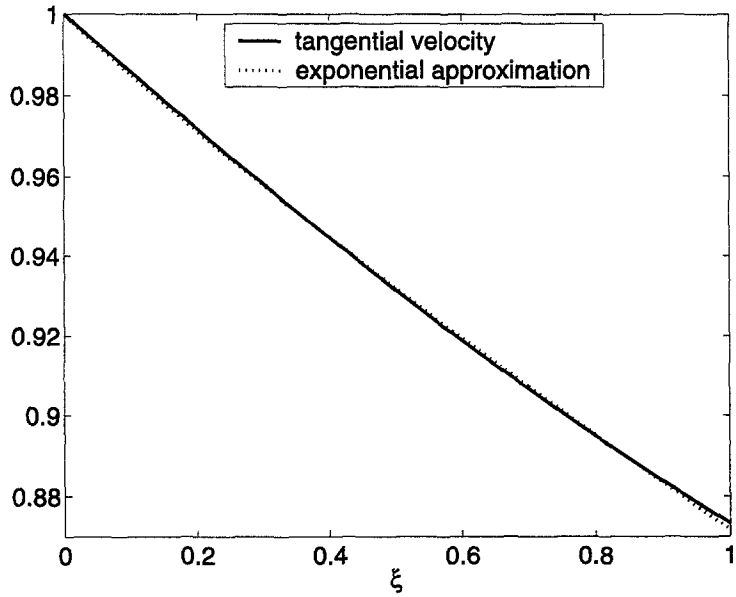

(a)

Figure 4. Function (24) and its exponential approximation according to Table 1, $[\xi_l, \xi_r] = [0, 1]$ (a), $[\xi_l, \xi_r] = [0, 100]$ (b), $U_\infty = 2$.

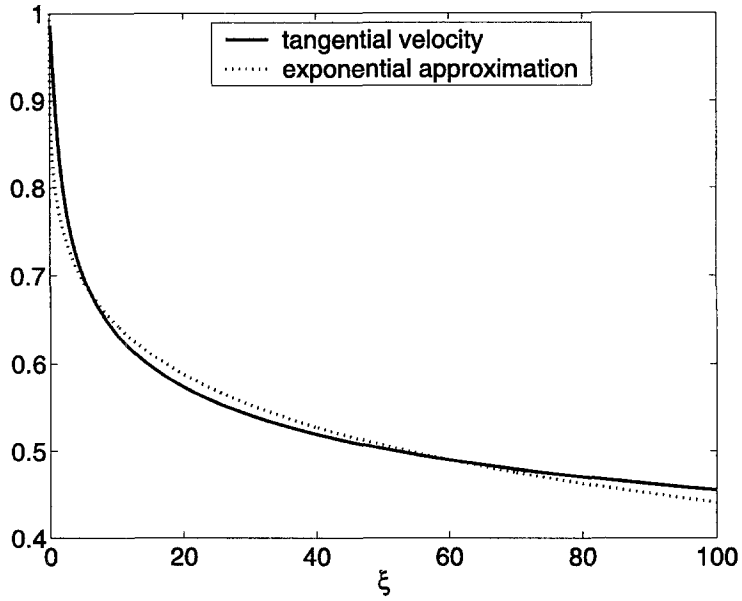

(b)

Figure 4. (cont.)

5. A NUMERICAL ILLUSTRATION

It is known that in flows with potential body forces and laminar initial conditions all vorticity is generated at the boundary. Thus, practical turbulent flow simulations only need to replicate three effects:

(1) generation of eddies at walls,
(2) interaction of eddies, and
(3) decay of eddies.

Obviously, the wall model used has the most critical role in the first. Thus, we study herein a simple, underresolved flow with recirculation caused by flow-boundary interaction: the flow across a step. The most distinctive feature of this flow is a recirculating vortex behind the step, see Figures 8 and 9 for illustrations.

We will study the evolution of the position of the reattachment point of the recirculating eddy using a simple LES model—the Smagorinsky model. The only difference between the Navier-Stokes equations (NSE) and the Smagorinsky model (NSE + SMA) is in the viscous term. Whereas this term is $\nabla \cdot (2\,\mathrm{Re}^{-1}\,\mathbb{D}(\mathbf{u}))$ in the Navier-Stokes equations (1), it has the form

$$\nabla \cdot \left(\left(2\,\mathrm{Re}^{-1} + c_S \delta^2 \, \|\mathbb{D}(\mathbf{u})\|_F \right) \mathbb{D}(\mathbf{u}) \right)$$

in the Smagorinsky model. Here, c_S is a positive constant (usually $c_S \approx 0.01$, see [1]) and $\|\cdot\|_F$ denotes the Frobenius norm of a tensor. We used $c_S = 0.01$ in the computations presented in this section. Although the Smagorinsky model is widely used, it has some drawbacks. These are well documented in the literature, e.g., see [19]. For instance, the Smagorinsky model constant c_S is an *a priori* input and this single constant is not capable of representing correctly various turbulent flows. Another drawback of this model is that it introduces too much diffusion into the flow, e.g., see [20] or Figures 8 and 9. However, keeping the closure model fixed and testing various NWMs leads to valid conclusions while varying both would lead to a lot of data with no clean comparison.

The domain of the two-dimensional flow across a step is presented in Figure 5. Here we present results for a parabolic inflow profile, which is given by $\mathbf{u} = (u, v)^\top$, with $u = y(10 - y)/25$, $v = 0$.

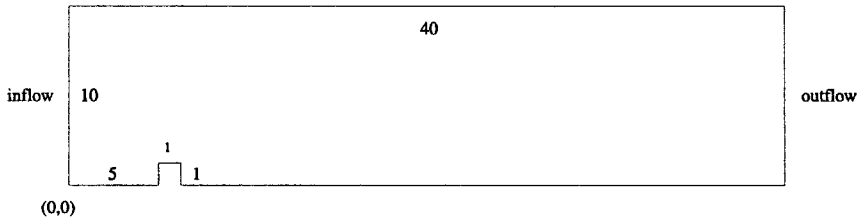

Figure 5. Domain of two-dimensional channel with a step.

Boundary condition (3) is prescribed on the top and bottom boundary as well as on the step. The flow leaves the domain by an outflow boundary condition on the right side of the channel. The reattachment point is defined by the change of the sign of the tangential velocity on the bottom boundary. The Smagorinsky model was applied with no-slip boundary conditions (NSE + SMA + NOSLIP) and with boundary condition (3) (NSE + SMA + SWF).

The computations were performed on various grids. For instance, for the fully resolved NSE + NOSLIP simulation, which is our "truth" solution, we used a fine grid whereas a much coarser grid has been used for NSE + SMA + SWF, NSE + SMA + NOSLIP, and NSE + SWF. The point is obviously to compare the performance of the various options in underresolved simulations by comparison against a "truth"/fully-resolved solution.

The computations were performed with the code MooNMD; see [21,22] for descriptions of its basic components. The Navier-Stokes equations and the Smagorinsky model were discretized in time with the fractional-step θ-scheme (an implicit scheme of second order) and in space with the Q_2/P_1^{disc} finite-element method, i.e., the velocity is approximated by continuous piecewise biquadratics and the pressure by discontinuous piecewise linears. The coarse grid which was used in the computations (level 1) is given in Figure 6. The number of degrees of freedom on this grid is 2202 for the velocity and 768 for the pressure. The fine grid computations were performed on the grid which is obtained from the coarse grid after two uniform refinement steps (level 3). On this grid, there are 33,378 velocity degrees of freedom and 12,288 pressure degrees of freedom.

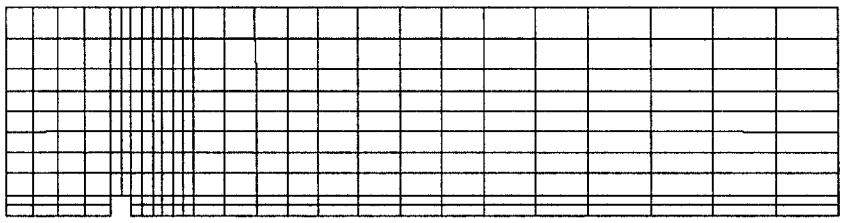

Figure 6. Two-dimensional channel with a step, coarsest mesh (level 1).

The results pictured in Figure 7 give strong, although admittedly very preliminary, support for the general form of the NWM. Indeed, the NSE + SMA + SWF test replicates exactly the reattachment length until the true eddy separates (just before $t = 10$) and the Smagorinsky eddy remains attached. Most remarkably, the underresolved NSE + SWF simulation produces over time a more accurate description of the reattachment length than the NSE + SMA + NOSLIP simulation.

Clearly, the Smagorinsky model is too stabilizing: eddies which should separate and evolve remain attached and attain steady state. However, regarding the main point of study, the NWM (3), it is also clear that this NWM improved the estimate of the reattachment length in all simulations. Further studies and tests of this approach are thus well merited!

APPENDIX

The Appendix provides a collection of some formulas which have been used in the derivation and the analysis of the friction coefficients.

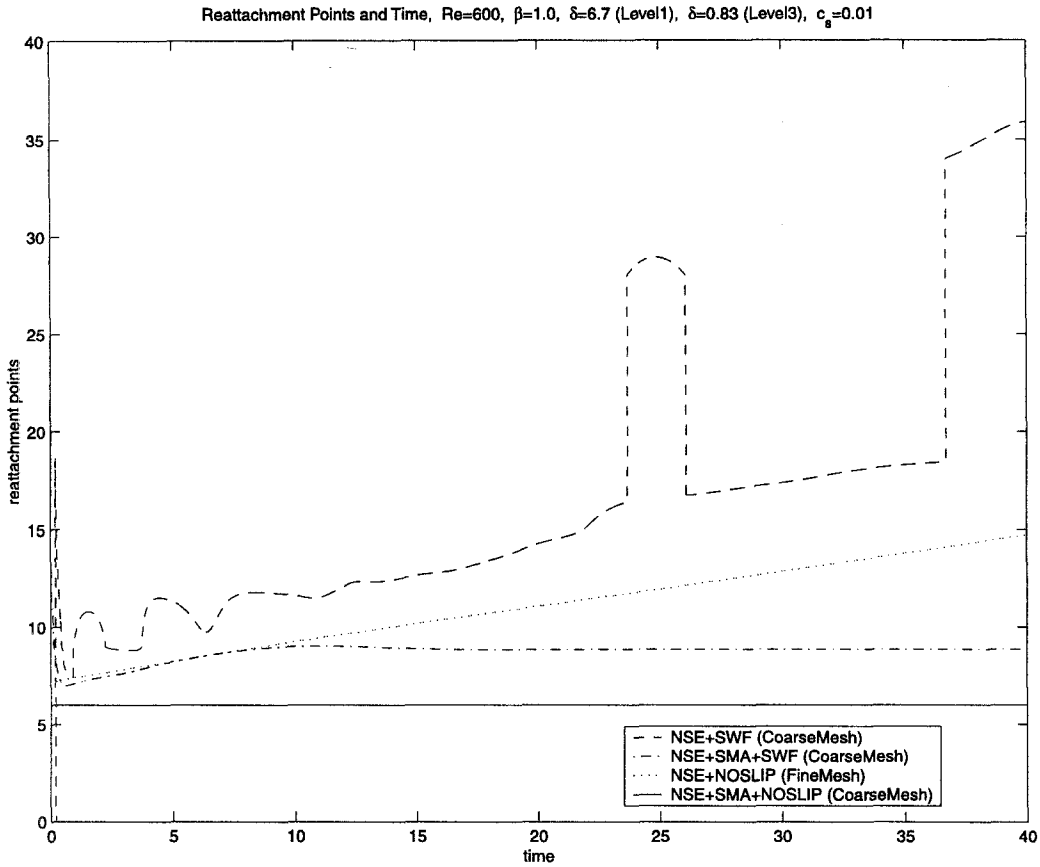

Figure 7. Evolution of the reattachment points, Re = 600.

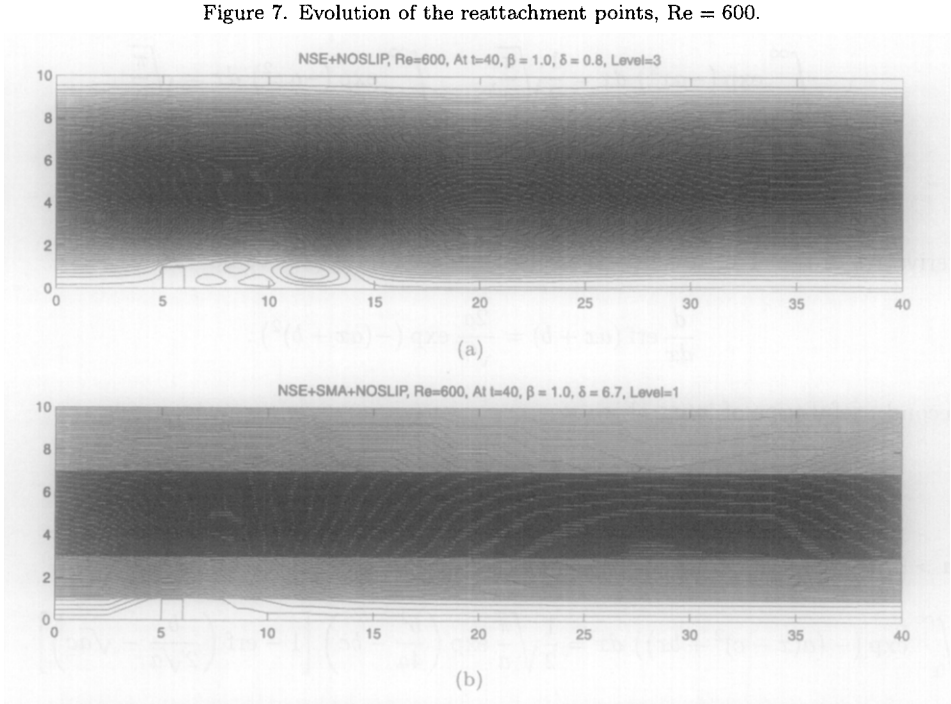

Figure 8. Two-dimensional channel with a step, the streamlines of the solution for NSE + NOSLIP on the finest mesh (a) and NSE + SMA + NOSLIP on the coarsest mesh (b) at time $t = 40$, Re = 600.

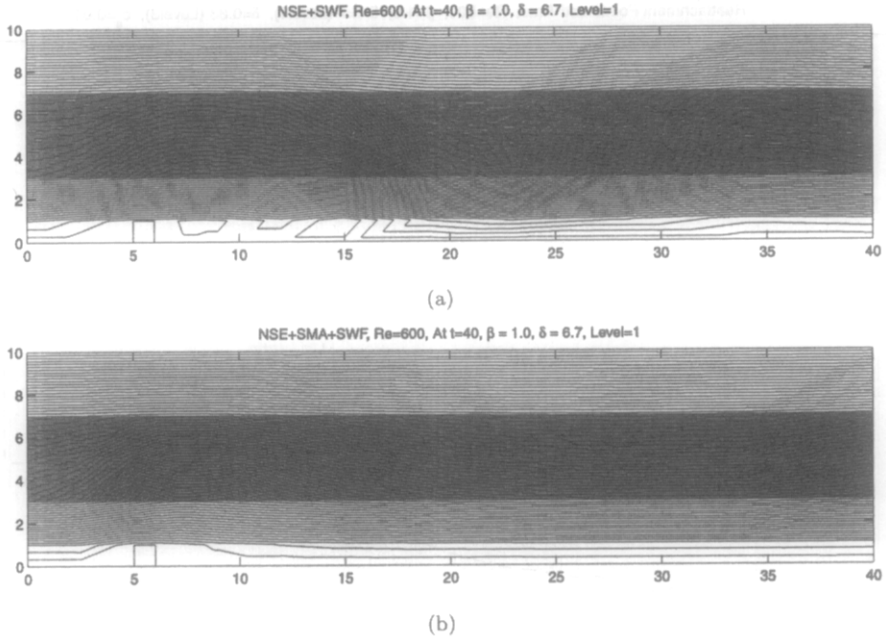

Figure 9. Two-dimensional channel with a step, the streamlines of the solution for NSE + SWF on the coarsest mesh (left) and NSE + SMA + SWF on the coarsest mesh (right) at time $t = 40$, Re $= 600$.

It holds

$$\int_0^b \exp\left(-ax^2\right)\, dx = \frac{1}{2}\sqrt{\frac{\pi}{a}}\,\mathrm{erf}\left(b\sqrt{a}\right), \qquad a > 0, \tag{26}$$

where erf $(\cdot)$ denotes the error function. Recall that

$$\int_0^\infty \exp\left(-ax^2\right)\, dx = \frac{1}{2}\sqrt{\frac{\pi}{a}}, \qquad \int_{-\infty}^\infty \exp\left(-ax^2\right)\, dx = \sqrt{\frac{\pi}{a}} \tag{27}$$

and

$$\int_0^\infty \exp\left(-a(x-b)^2\right)\, dx = \frac{1}{2}\sqrt{\frac{\pi}{a}}\left(1 + \mathrm{erf}\left(b\sqrt{a}\right)\right). \tag{28}$$

The derivative of the error function is easily calculated from (26) to be

$$\frac{d}{dx}\,\mathrm{erf}\,(ax+b) = \frac{2a}{\sqrt{\pi}}\exp\left(-(ax+b)^2\right). \tag{29}$$

A second useful type of integral is

$$\int_0^\infty \exp\left(-\left(ax^2+bx+c\right)\right)\, dx = \frac{1}{2}\sqrt{\frac{\pi}{a}}\exp\left(\frac{b^2-4c}{4a}\right)\left[1 - \mathrm{erf}\left(\frac{b}{2\sqrt{a}}\right)\right], \tag{30}$$

with $a > 0$, see [23, Chapter 7.4]. It follows that

$$\int_0^\infty \exp\left(-\left(a(x-c)^2+bx\right)\right)\, dx = \frac{1}{2}\sqrt{\frac{\pi}{a}}\exp\left(\frac{b^2}{4a} - bc\right)\left[1 - \mathrm{erf}\left(\frac{b}{2\sqrt{a}} - \sqrt{a}c\right)\right]. \tag{31}$$

The third type of integral which will be needed has the form

$$\int_0^b \exp\left(-ax^2\right) x^c\, dx, \qquad \text{with } a, b > 0, \quad c > -1.$$

The substitution $t = ax^2$ yields

$$\int_0^b \exp\left(-ax^2\right) x^c \, dx = \frac{1}{2} a^{-(c+1)/2} \int_0^{ab^2} \exp(-t) t^{(c+1)/2-1} \, dt. \tag{32}$$

This integral can be evaluated by the Gamma function $\Gamma(d)$ and the incomplete Gamma function $\Gamma(d, x)$. By the definition of the incomplete Gamma function, see [23, Chapter 6.5], we have

$$\Gamma(d, x) = \Gamma(d) - \int_0^x \exp(-t) t^{d-1} \, dt, \qquad d > 0. \tag{33}$$

Combining (32) and (33) gives

$$\int_0^b \exp\left(-ax^2\right) x^c \, dx = \frac{1}{2} a^{-(c+1)/2} \left[\Gamma\left(\frac{c+1}{2}\right) - \Gamma\left(\frac{c+1}{2}, ab^2\right)\right]. \tag{34}$$

REFERENCES

1. P. Sagaut, *Large Eddy Simulation for Incompressible Flows*, Springer-Verlag, Berlin, (2001).
2. V. John and W.J. Layton, Analysis of numerical errors in large eddy simulation, *SIAM J. Numer. Anal.* **40**, 995–1020, (2002).
3. S.B. Pope, *Turbulent Flows*, Cambridge University Press, (2000).
4. J.S. Baggett, F. Nicaud, T. Bewley, J. Gullbrand and O. Botella, Suboptimal control based wall models for LES—Including transpiration velocity, In *Proc. 2000 Summer Program*, pp. 331–342, Center Turbul. Res., Stanford University, CA, (2000).
5. O.V. Vasilyev, T.S. Lund and P. Moin, A general class of commutative filters for LES in complex geometries, *Journal of Computational Physics* **146**, 82–104, (1998).
6. G.P. Galdi and W.J. Layton, Approximation of the larger eddies in fluid motion II: A model for space filtered flow, *Math. Models and Meth. in Appl. Sciences* **10** (3), 343–350, (2000).
7. C.L.M.H. Navier, Mémoire sur les lois du mouvement des fluiales, *Mém. Acad. Royal Society* **6**, 389–440, (1823).
8. J.C. Maxwell, *Phil. Trans. Royal Society*, (1879).
9. V. John, Slip with friction and penetration with resistance boundary conditions for the Navier-Stokes equations—Numerical tests and aspects of the implementation, *J. Comp. Appl. Math.* **147**, 287–300, (2002).
10. T. Iliescu, V. John and W.J. Layton, Convergence of finite element approximations of large eddy motion, *Num. Meth. Part. Diff. Equ.* **18**, 689–710, (2002).
11. T. Clopeau, A. Mikelic and R. Robert, On the vanishing viscosity limit for the 2d incompressible Navier-Stokes equations with the friction type boundary conditions, *Nonlinearity* **11**, 1625–1636, (1998).
12. C. Parés, Approximation de la solution des equations d'un modele de turbulence par une methode de Lagrange-Galerkin, *Rev. Mat. Apl.* **15**, 63–124, (1994).
13. A. Liakos, Weak imposition of boundary conditions in the Stokes and Navier-Stokes equation, Ph.D. Thesis, Univ. of Pittsburgh, (1999).
14. J.S. Smagorinsky, General circulation experiments with the primitive equations, *Mon. Weather Review* **91**, 99–164, (1963).
15. T. Knopp, Finite-element simulation of buoyancy-driven turbulent flows, Ph.D. Thesis, Univ. of Göttingen, Germany, (2003).
16. H. Schlichting, *Boundary-Layer Theory*, McGraw-Hill, New York, (1979).
17. W.J. Layton, Weak imposition of "no-slip" conditions in finite element methods, *Computers Math. Applic.* **38**, 129–142, (1999).
18. G.I. Barenblatt and A.J. Chorin, New perspectives in turbulence: Scaling laws, asymptotics, and intermittency, *SIAM Review* **40** (2), 265–291, (1998).
19. Y. Zang, R.L. Street and J.R. Koseff, A dynamics mixed subgrid-scale model and its application to turbulent recirculating flows, *Phys. Fluids A* **5**, 3186–3196, (1993).
20. T. Iliescu, V. John, W.J. Layton, G. Matthies and L. Tobiska, A numerical study of a class of LES models, *Int. J. Comput. Fluid Dyn.* **17**, 75–85, (2003).
21. V. John, *Large Eddy Simulation of Turbulent Incompressible Flows. Analytical and Numerical Results for a Class of LES Models*, Volume 34 of Lecture Notes in Computational Science and Engineering, Springer-Verlag, Berlin, (2003).
22. V. John and G. Matthies, MooNMD—A program package based on mapped finite element methods, *Comput. Visual. Sci.* **6**, 163–170, (2004).
23. M. Abramowitz and I.A. Stegun, *Handbook of Mathematical Functions, with Formulas, Graphs, and Mathematical Tables*, 9th edition, Dover, New York, (1965).